

This discussion paper is/has been under review for the journal *Atmospheric Chemistry and Physics (ACP)*. Please refer to the corresponding final paper in *ACP* if available.

# Evidence for ice particles in the tropical stratosphere from in-situ measurements

**M. de Reus<sup>1,2</sup>, S. Borrmann<sup>1,2</sup>, A. J. Heymsfield<sup>3</sup>, R. Weigel<sup>4</sup>, C. Schiller<sup>5</sup>,  
V. Mitev<sup>6</sup>, W. Frey<sup>2</sup>, D. Kunkel<sup>2</sup>, A. Kürten<sup>7</sup>, J. Curtius<sup>8</sup>, N. M. Sitnikov<sup>9</sup>,  
A. Ulanovsky<sup>9</sup>, and F. Ravagnani<sup>10</sup>**

<sup>1</sup>Max Planck Institute for Chemistry, Particle Chemistry Department, Mainz, Germany

<sup>2</sup>Institute for Atmospheric Physics, Mainz University, Germany

<sup>3</sup>National Center for Atmospheric Research, Boulder, USA

<sup>4</sup>Laboratoire de Météorologie Physique, Université Blaise Pascal, Clermont-Ferrand, France

<sup>5</sup>Institute of Chemistry and Dynamics of the Geosphere, Research Centre Jülich, Germany

<sup>6</sup>Swiss Centre for Electronics and Microtechnology, Neuchâtel, Switzerland

<sup>7</sup>Div. of Engineering and Applied Science California Inst. of Technology, Pasadena, Ca., USA

<sup>8</sup>Institute for Atmospheric and Environmental Sciences, Goethe Univ. of Frankfurt, Germany

<sup>9</sup>Central Aerological Observatory, Dolgoprudny, Moskow Region, Russia

<sup>10</sup>Institute of Atmospheric Sciences and Climate, Bologna, Italy

Received: 19 August 2008 – Accepted: 24 September 2008 – Published: 14 November 2008

Correspondence to: M. de Reus (reus@mpch-mainz.mpg.de)

Published by Copernicus Publications on behalf of the European Geosciences Union.

## Ice particles in the tropical stratosphere

M. de Reus et al.

Title Page

Abstract

Introduction

Conclusions

References

Tables

Figures

◀

▶

◀

▶

Back

Close

Full Screen / Esc

Printer-friendly Version

Interactive Discussion



## Abstract

In-situ ice crystal size distribution measurements are presented within the tropical troposphere and lower stratosphere. The measurements were performed using a combination of a Forward Scattering Spectrometer Probe (FSSP-100) and a Cloud Imaging Probe (CIP) which were installed on the Russian high altitude research aircraft M55 “Geophysica” during the SCOUT-O<sub>3</sub> campaign in Darwin, Australia. The objective of the campaign was to characterise the outflow of the Hector convective system, which appears on an almost daily basis during the pre-monsoon season over the Tiwi Islands, north of Darwin. In total 90 encounters with ice clouds, between 10 and 19 km altitude were selected from the dataset and were analysed. Six of these encounters were observed in the lower stratosphere, up to 1.4 km above the local tropopause, and were a result of overshooting convection. The ice crystals observed in the stratosphere comprise sizes up to 400  $\mu\text{m}$  maximum dimension, include an ice water content of  $0.1 \times 10^{-3}$ – $1.7 \times 10^{-3} \text{ g m}^{-3}$  and were observed at ambient relative humidities (with respect to ice) between 75 and 157%. Three modal lognormal size distributions were fitted to the average size distributions for different potential temperature intervals, showing that the shape of the size distribution of the stratospheric ice clouds are similar to those observed in the upper troposphere.

In the tropical troposphere the effective radius of the ice cloud particles decreases from 100  $\mu\text{m}$  at about 10 km altitude, to 3  $\mu\text{m}$  at the tropopause, while the ice water content decreases from 0.04 to  $10^{-5} \text{ g m}^{-3}$ . No clear trend in the number concentration was observed with altitude, due to the thin and inhomogeneous characteristics of the observed cirrus clouds.

The ice water content calculated from the observed ice crystal size distribution is compared to the ice water content derived from two hygrometer instruments. This independent measurement of the ice water content agrees within the combined uncertainty of the instruments for ice water contents exceeding  $2 \times 10^{-4} \text{ g m}^{-3}$ .

Stratospheric residence times, calculated based on gravitational settling only, show

## Ice particles in the tropical stratosphere

M. de Reus et al.

Title Page

Abstract

Introduction

Conclusions

References

Tables

Figures

◀

▶

◀

▶

Back

Close

Full Screen / Esc

Printer-friendly Version

Interactive Discussion



that the ice crystals observed in the stratosphere over the Hector storm system have a high potential for humidifying the stratosphere.

Utilizing total aerosol number concentration measurements from a four channel condensation particle counter, it can be shown that the fraction of activated ice particles with respect to the number of available aerosol particles ranges from 1:300 to 1:30 000 for tropical upper tropospheric ice clouds with ambient temperatures below  $-75^{\circ}\text{C}$ .

## 1 Introduction

Cirrus clouds play a significant role in regulating the radiation balance of the Earth-atmosphere system and are, hence, an important component of the Earth's climate system. Cirrus clouds can absorb outgoing terrestrial radiation, and thereby act as a greenhouse gas (warming the atmosphere). At the same time, they can reflect incoming solar radiation back to space and cause a cooling of the atmosphere. Which process dominates and, hence, the arithmetic sign of the net radiative forcing of cirrus clouds, appears to be very sensitive to the cloud microphysical and macrophysical properties (Lynch et al., 2002). For example, thin cirrus clouds cause a small but positive radiative forcing at the top of the atmosphere, whereas thick cirrus clouds may cause cooling (Stephens and Webster, 1981).

Cirrus clouds can also alter the chemical composition of the tropopause region by uptake of water and nitric acid (Voigt et al., 2006), while heterogeneous reactions of halogen species on the surface of cirrus particles can affect the ozone budget of the tropopause region (Borrmann et al., 1996).

Moreover, cirrus clouds are involved in vertical transport as well as hydration and dehydration of airmasses. Cloud droplets and water vapour enter the upper free troposphere by convection and are further transported into the stratosphere by a slower radiatively driven ascent, giving the airmass enough time to dehydrate by condensation and subsequent sedimentation of ice particles (Sherwood and Dessler, 2001). Over-shooting convection penetrating directly into the stratosphere, however, might hydrate

## Ice particles in the tropical stratosphere

M. de Reus et al.

Title Page

Abstract

Introduction

Conclusions

References

Tables

Figures



Back

Close

Full Screen / Esc

Printer-friendly Version

Interactive Discussion



the stratosphere (Chaboureau et al., 2007; Corti et al., 2008) and thereby contribute to the observed increase in stratospheric water vapour concentrations (Oltmans et al., 2000).

In order to quantify the radiative effect of cirrus clouds and their influence on the water budget and air chemistry, detailed information about their microphysical properties are necessary. Measurements within cirrus clouds show a wide range of particle shapes, sizes, and concentrations (Heymsfield and McFarquhar, 2002; Schiller et al., 2008). Below, examples of in-situ cirrus particle size distribution measurements are given at mid-latitudes and in the tropics, in the troposphere as well as in the stratosphere.

During the INCA (INterhemispheric differences in Cirrus properties from Anthropogenic emissions) project, cirrus measurements were performed in the northern and southern hemisphere at mid-latitudes up to 12 km altitudes. In the northern hemisphere ice crystals were found to be smaller and associated with higher ice crystal number concentrations compared to the southern hemisphere. The mean ice crystal concentration was  $2.2 \text{ cm}^{-3}$  in the NH and  $1.4 \text{ cm}^{-3}$  in the SH, with an effective diameter of  $36 \mu\text{m}$  and  $42 \mu\text{m}$ , respectively. No significant differences in the ice water content and ice crystal shape were observed (Gayet et al., 2004). This is in agreement with mid-latitude Northern Hemisphere measurements presented by Ström et al. (1997). They observed a median ice crystal concentration of  $2.6 \text{ cm}^{-3}$ , while the crystal number distribution peaks at diameters below  $10 \mu\text{m}$ . However, artefacts by shattering on the inlet in these datasets cannot be excluded.

Size distributions of cirrus clouds in the upper tropical troposphere, exhibiting a pronounced peak at  $10 \mu\text{m}$ , have been reported by Thomas et al. (2002). They found very thin layers of subvisible cirrus clouds in the outflow of a cumulonimbus cloud, with ice crystal number concentrations ranging between 0.04 and  $0.87 \text{ cm}^{-3}$ , depending on the exact position within the cirrus layer. McFarquhar et al. (2000) report on a similar thin subvisible cirrus layer over the tropical central Pacific, with a typical ice water content between  $10^{-6}$  and  $10^{-4} \text{ g m}^{-3}$ , maximum ice crystal sizes between 30 and  $140 \mu\text{m}$ , and a cloud radiative forcing up to  $5 \text{ Wm}^{-2}$ . Moreover, ultrathin tropical

**Ice particles in the tropical stratosphere**

M. de Reus et al.

Title Page

Abstract

Introduction

Conclusions

References

Tables

Figures

◀

▶

◀

▶

Back

Close

Full Screen / Esc

Printer-friendly Version

Interactive Discussion



**Ice particles in the  
tropical stratosphere**

M. de Reus et al.

[Title Page](#)[Abstract](#)[Introduction](#)[Conclusions](#)[References](#)[Tables](#)[Figures](#)[I◀](#)[▶I](#)[◀](#)[▶](#)[Back](#)[Close](#)[Full Screen / Esc](#)[Printer-friendly Version](#)[Interactive Discussion](#)

tropospheric clouds (UTTC) were observed directly beneath the tropical tropopause, characterised by a very low ice crystal number concentration ( $0.05 \text{ cm}^{-3}$ ). The different cirrus clouds reported in this study, all show a peak in the ice crystal number size distribution at about  $10 \mu\text{m}$  diameter. These ultrathin tropical tropospheric clouds may exist for many hours as an only 200–300 m thick cloud layer just a few hundred meters below the tropical cold point tropopause covering up to  $10\,000 \text{ km}^2$  (Peter et al., 2003). In-situ measurements of cirriform clouds in the upper tropical troposphere have been reported by Heymsfield (1986), who found ice crystals (trigonal plates and columns) with sizes up to  $50 \mu\text{m}$  at temperatures of  $-83^\circ\text{C}$  and Knollenberg et al. (1993) who found high concentrations of ice crystals ( $>10 \text{ cm}^{-3}$ ) in the anvils of tropical convective systems.

Ice crystals have also been observed in the stratosphere. Besides polar stratospheric clouds, which are observed at cold temperatures over the Arctic and Antarctic, ice crystals have been observed in the tropical stratosphere as well. The presence of clouds in the tropical stratosphere has been attributed to overshooting convection (Chaboureau et al., 2007; Nielsen et al., 2007; Corti et al., 2008).

This paper shows direct evidence from in-situ measurements for the presence of ice crystals in the tropical stratosphere, immediately above a large convective system, indicating direct transport of cloud particles from the troposphere to the stratosphere. Unique in-situ measurements of the cloud particle size distribution ranging from  $3 \mu\text{m}$  to  $1.5 \text{ mm}$  diameter are presented. Moreover, vertical profiles of the total and non-volatile aerosol number concentration are shown and a relationship between the number of measured ice cloud particles with respect to the available aerosol particles larger than  $10 \text{ nm}$  is presented.

## 2 Experiment and instrumentation

### 2.1 The SCOUT-O<sub>3</sub> pre-monsoon in Darwin, Australia, 2005

During November and December 2005 four aircraft were stationed in Darwin, Australia for a combined mission of the SCOUT-O<sub>3</sub> (Stratospheric-Climatic Links with Emphasis on the Upper Troposphere and Lower Stratosphere) and ACTIVE (Aerosol and Chemical Transport in Tropical Convection) projects. The main goal of the mission was to investigate the transport and transformation of water vapour, aerosol and trace gases in deep convection. Darwin was chosen as the aircraft base for the mission because of the Hector storm system, which appears on an almost daily basis over the Tiwi Islands, north of Darwin, during the pre-monsoon season in November and December (Connolly et al., 2006). The storms generated over the islands can reach heights up to 20 km. Hence, Hector events could play an important role in vertical transport of mass and pollutants into the tropical tropopause layer and possibly the lowermost stratosphere. An overview of the objectives, measurement platforms, instrumentation and performed flights during the SCOUT-O<sub>3</sub>/ACTIVE campaign is presented by Vaughan et al. (2008), while the meteorological situation is described in detail by Brunner et al. (2008).

As part of the SCOUT-O<sub>3</sub> project nine flights were performed with the high altitude research aircraft M55 “Geophysica”. Ice crystal size distributions were measured on-board the “Geophysica” using two instruments: a modified Particle Measuring Systems (PMS) Forward Scattering Spectrometer Probe (FSSP-100) with Droplet Measurement Technologies (DMT) high speed electronics (SPP-100) and a DMT Cloud Imaging Probe (CIP).

Title Page

Abstract

Introduction

Conclusions

References

Tables

Figures

◀

▶

◀

▶

Back

Close

Full Screen / Esc

Printer-friendly Version

Interactive Discussion



## 2.2 Modified FSSP-100 for cloud particle size distribution measurements ( $2.7 < D_p < 31 \mu\text{m}$ )

The FSSP-100 measures the forward scattering of single particles within a scattering angle of  $3\text{--}15^\circ$  (Dye and Baumgardner, 1984). Using Mie-calculations, the size of a particle is related to the measured scattering cross section, which implicitly assumes spherical particles. However, at least for the diameter range from  $0.3$  to  $16 \mu\text{m}$  it was shown by means of T-matrix calculations (Borrmann et al., 2000) that aspherical particles can be detected and reliably sized by FSSP-type optical particle counters with the given forward scattering geometry. Since this study focuses on stratospheric ice crystals, the refractive index of ice has been used. The settings of the instrument during the SCOUT- $\text{O}_3$  project allowed the determination of the ice crystal size distribution in 40 size bins between  $2.7$  and  $31 \mu\text{m}$  diameter ( $D_p$ ). Due to ambiguities in the Mie scattering curve and the low observed ice crystal number concentrations, the size distributions presented in this paper have been comprehended into 7 size bins.

The uncertainty of the ice crystal number concentration measured by the FSSP is mainly determined by the uncertainty in the sample volume, which has been estimated to be 20% (Baumgardner et al., 1992). At low particle number concentrations the uncertainty due to counting statistics has to be taken into account, which is defined as the square root of the number of particles measured. Secondly, it has been recognized that shattering of large ice crystals on the housing of the FSSP and CIP probe may produce large numbers of small particles, which, under certain circumstances, can lead to incorrect measurements of particle size distributions and subsequently derived microphysical properties (McFarquhar et al., 2007). Due to the relatively low ice crystal number concentrations and small ice crystals observed in the upper tropical troposphere and lower stratosphere, it is not likely that shattering has significantly influenced the measurements presented in this study. This will be discussed in detail in Sect. 5.2.

For calculating the particle volume and mass concentration, additionally the uncer-

Title Page

Abstract

Introduction

Conclusions

References

Tables

Figures

◀

▶

◀

▶

Back

Close

Full Screen / Esc

Printer-friendly Version

Interactive Discussion



tainty in the particle sizing is important, which is dependent on particle shape, ambiguities in the Mie curve and uncertainties in the refractive index of the particles. Baumgardner et al. (1992) estimated the overall uncertainty of the FSSP volume concentration measurements to be 60%. Uncertainties due to coincidence are not important for the ice clouds analysed in this paper due to the very low ice crystal number concentration.

### 2.3 CIP for cloud particle size distribution measurements ( $25 < D_p < 1550 \mu\text{m}$ )

The CIP is a two dimensional optical array probe following the initial design from Knollenberg et al. (1970). Two dimensional shadow images of particles are obtained by a linear array of 64 light detectors as they obscure a laser beam at a rate proportional to the airspeed. At  $190 \text{ms}^{-1}$ , the typical cruising speed of the Geophysica in the upper troposphere and lower stratosphere, this corresponds to a sampling rate of 8 MHz. Each sample of the 64 elements, is called a slice; up to 62 slices compose a particle image. The resolution of the resulting particle image is  $25 \times 25 \mu\text{m}$ , leading to a detectable particle size range of  $25\text{--}1550 \mu\text{m}$  ( $62 \times 25 \mu\text{m}$ ). Due to an underestimation of the airspeed measured by the CIP probe itself, the real resolution was  $25 \times 35 \mu\text{m}$  during this project, which has been corrected for.

From the recorded images the particle size has been deduced using two different size definitions: the minimum and the maximum dimension, which are defined as the diameter of a circle with the same surface area as the shaded area of the image and the maximum chord length within the particle, respectively. For spherical particles, these two diameters are almost identical.

Incidences of shattering have been removed from the CIP dataset by using a threshold interarrival time of  $10^{-5} \text{s}$  (Field et al., 2006). This method assumes that shattering of a large ice crystal causes a burst of small particles with very short interarrival times, which can be distinguished from the longer interarrival times of real cloud particles in a cirrus cloud.

Particles shading the first or the last diode of the array are removed from the dataset.

## Ice particles in the tropical stratosphere

M. de Reus et al.

Title Page

Abstract

Introduction

Conclusions

References

Tables

Figures

◀

▶

◀

▶

Back

Close

Full Screen / Esc

Printer-friendly Version

Interactive Discussion



**Ice particles in the tropical stratosphere**

M. de Reus et al.

[Title Page](#)[Abstract](#)[Introduction](#)[Conclusions](#)[References](#)[Tables](#)[Figures](#)[◀](#)[▶](#)[◀](#)[▶](#)[Back](#)[Close](#)[Full Screen / Esc](#)[Printer-friendly Version](#)[Interactive Discussion](#)

Since mainly small particles ( $D_p < 400 \mu\text{m}$ ) were observed in this project, this will not lead to a high rejection rate of observed particles. Moreover, particles are rejected when the ratio of the shaded area of the particles over the area of a circle with the maximum dimension is below 0.1. This eliminates many bad particles, for example “streakers” which are caused by splash or shatter products travelling slower than the true airspeed through the sample volume. This rejection criterion also removes most of the images containing two particles.

The CIP starts recording the image as soon as one of the diodes gets shaded, which leads to the loss of the first slice of each particle image. This lost slice has been reconstructed by removing a pixel from each edge of the recorded first slice, until at least half of the pixels are gone. This slice is inserted as slice zero in the image.

Image frames which show no shaded pixels are assumed to have triggered the data acquisition program, but only left a signal in the first, non recorded, slice. These particles are assumed to have a maximum dimension of  $43 \mu\text{m}$  (1 pixel of  $25 \times 35 \mu\text{m}$ ).

No correction for out of focus particles has been done. While a correction has been developed for liquid cloud droplets, its applicability to ice crystals is questionable. Since, the size of out of focus particles is overestimated, this will lead to a shift of the size distribution to larger sizes.

Analogous to the FSSP, the uncertainty in the particle number concentration measured with the CIP is mainly determined by the uncertainty in the sample volume and for low particle concentrations by counting statistics. The sample volume has been calculated using the entire-in method described by Heymsfield and Parrish (1978). The sample volume increases with increasing particle size, thus compensating for the decrease in concentration with increasing crystal size. The uncertainty in the sample volume is estimated to be 20%, similar as for the FSSP. Additional uncertainty in the sample volume is caused by the relatively high aircraft speed of the Geophysica aircraft (up to  $200 \text{ms}^{-1}$ ), due to the non-zero electronic response time of the CIP instrument (Baumgardner and Korolev, 1997).

In order to calculate the particle size distribution and volume concentration, the un-

**Ice particles in the tropical stratosphere**

M. de Reus et al.

[Title Page](#)[Abstract](#)[Introduction](#)[Conclusions](#)[References](#)[Tables](#)[Figures](#)[◀](#)[▶](#)[◀](#)[▶](#)[Back](#)[Close](#)[Full Screen / Esc](#)[Printer-friendly Version](#)[Interactive Discussion](#)

certainty in the particle size has to be taken into account. The uncertainty in the particle size decreases considerably with particle size and is  $\pm 25 \mu\text{m}$  for particles  $> 50 \mu\text{m}$  diameter. The intensity of the laser light on a diode has to decline by more than 50% to be recorded as shaded. This means that theoretically a  $25 \mu\text{m}$  particle which passes exactly over the middle of two diodes will be recorded as a  $50 \mu\text{m}$  particle, but also a  $74.9 \mu\text{m}$  particle will be interpreted as a  $50 \mu\text{m}$  particle when it shadows two diodes completely and two for only 49.8%. For the first particle size bin, with a nominal size of  $25 \mu\text{m}$  diameter, particles could have a diameter between 12.5 and  $49.9 \mu\text{m}$ . The non-zero response time of the photodiodes causes an additional uncertainty in the measured particle size at high airspeed (Strapp et al., 2001). Moreover, the particle diameter depends on the chosen definition of the particle size. To demonstrate this uncertainty, the ice crystal size distribution using the minimum and maximum dimension of the particle are shown.

#### 2.4 Combined number and mass size distributions from the modified FSSP-100 and the CIP

In this paper data of the FSSP and CIP are combined to attain ice crystal size distributions for particles with a diameter between  $3 \mu\text{m}$  to 1.5 mm. Figure 1 shows an example of a combined size distribution which was observed in the stratosphere, 0.7 km above the local tropopause, over the Tiwi islands on 30 November 2005 (see Sect. 3.3). Additionally, the interarrival time distribution, for the ice crystals observed by the CIP, is shown for this time period, indicating the different distributions of the ice crystals in natural cirrus clouds and shattered crystals. During the selected time period 3009 ice crystals were recorded by the CIP. From these, 199 particles are rejected based on the interarrival time criterion (6.6%), 15 (0.5%) because their area ratio was smaller than 0.1 and 347 (11.5%) while the shadow image touched one of the end diodes. Note that ice crystal images can be rejected by different criteria at the same time. The ice crystal size distribution measured by the CIP, shown in Fig. 1, is therefore based on a total of 2479 ice crystals, which is 82% of the total recorded images during this time period.

The FSSP counted 938 ice crystals during the same time period, which nevertheless result in higher concentrations as have been observed by the CIP, because of the up to 10 times smaller sample volume of the FSSP compared to the CIP.

A good agreement between the CIP and FSSP in the overlap region was observed during this time period, which was, however, not always the case. Note that the overlap region is very small and the uncertainty of the CIP for particles smaller than  $100\ \mu\text{m}$  is large due to the relatively large sizing uncertainty for this size range and potential losses of particles with sizes smaller than  $100\ \mu\text{m}$  (Korolev et al., 1998). A large difference in the size distribution can be observed for the different size definitions. In the remainder of this paper the maximum diameter is used for characterising the size of the ice crystals. The uncertainty in the measured number concentrations, which is displayed in Fig. 1 is the sum of the uncertainty in sample volume and counting statistics. For clarity reasons, in other graphs the error bars have been omitted.

## 2.5 Ice water content determination from hygrometer measurements

Besides calculating the ice water content from the observed ice crystal size distributions, the ice water content was also measured independently using two hygrometers. The total water content (gas-phase + particulate) has been measured using the Lyman- $\alpha$  hygrometer FISH (Fast In-Situ Hygrometer, Zöger et al., 1999), which is equipped with a forward facing inlet. Ice particles are over-sampled with an enhancement depending on altitude and cruising speed of the aircraft, which has been corrected for. For typical Geophysica cruising altitude and speed, the oversampling factor for particles with radii larger than  $4\ \mu\text{m}$  is 9 (Schiller et al., 2008). The accuracy of the FISH instrument is typically better than 6% and the precision is 0.2 ppm for water vapour mixing ratios of 3 ppm.

The gas phase water vapour content has been measured using the FLASH (FLuorescent Airborne Stratospheric Hygrometer) instrument (Sitnikov et al., 2007), with a measurement accuracy of 8%. The ice water content is determined by subtracting the water vapour content measured by FLASH from the total water content measured by

## Ice particles in the tropical stratosphere

M. de Reus et al.

Title Page

Abstract

Introduction

Conclusions

References

Tables

Figures

◀

▶

◀

▶

Back

Close

Full Screen / Esc

Printer-friendly Version

Interactive Discussion



the FISH instrument (see also Schiller et al., 2008).

## 2.6 Interstitial particle measurements using the COPAS instrument

The interstitial aerosol number concentration has been measured using two COndensation PARticle Counter Systems (COPAS). COPAS is a two channel aerosol counter designed for automated low pressure measurements of the particle number concentration (Curtius et al., 2005). One of the available four channels is heated to 250°C, causing volatile particles to evaporate (out of the detectable size range of the COPAS instrument) and only non-volatile particles to be counted. The other three channels are not heated but operated with different temperature settings, resulting in different 50% cut-off diameters of 6, 10 and 14 nm, respectively. The total aerosol number concentration for particles with diameters larger than 6, 10 and 14 nm is denoted as  $N_6$ ,  $N_{10}$  and  $N_{14}$ . The 50% cut off diameter of the heated channel is 10 nm, therefore, the particle number concentration measured by this channel is referred to as  $N_{10_{nv}}$ . The number concentration of particles with diameters between 6 and 14 nm ( $N_{6-14}$ ) has been obtained by subtracting  $N_{14}$  from  $N_6$ . These particles are so small that they are assumed to be recently formed in the atmosphere. They are often called ultrafine or nucleation mode particles.

## 2.7 Other instrumentation

Ozone mixing ratios have been determined using the Fast OZone ANalyzer (FOZAN), which is a chemiluminescence sensor operating with an accuracy of 0.01 ppm and a precision of 8% (Yushkov et al., 1999). The ambient temperature has been measured using a Thermo Dynamic Complex (TDC) probe with an accuracy of 0.5 K. Other parameters as position and true air speed have been adopted from the onboard navigational system UCSE (Unified Communications for Systems Engineer) of the “Geophysica” aircraft.

## Ice particles in the tropical stratosphere

M. de Reus et al.

Title Page

Abstract

Introduction

Conclusions

References

Tables

Figures

◀

▶

◀

▶

Back

Close

Full Screen / Esc

Printer-friendly Version

Interactive Discussion



### 3 Observations of ice crystals in the outflow of convective clouds

During the SCOUT-O<sub>3</sub> campaign nine flights were performed with the high altitude research aircraft M55 “Geophysica” from Darwin, Australia. Five flights focussed on in-situ measurements of the Hector storm system, while during the remaining four survey flights remote sensing of water vapour, cirrus, and trace gases was prioritised. During the Hector flights the aircraft did not penetrate the Hector storm system itself, because of aircraft safety reasons, but mainly probed the outflow from the storm system in the upper troposphere and lower stratosphere. During the survey flights measurements were performed in cirrus clouds as well, however they were not directly connected to the Hector storm system. The FSSP-100 was operated on all Hector flights and three survey flights, while the CIP provided reliable data on four Hector flights and one survey flight. In this paper we will focus on the five flights during which the FSSP and CIP instruments were operated simultaneously, i.e. the flights on 25, 28, 29 and 30 November (double flight) 2005.

During the selected flights, the tropopause height (defined by the in-situ measured cold point) varied in altitude between 16.8 and 18 km, partly because of the vicinity of the strong convective system. This corresponds to a cold point temperature ranging between  $-84$  and  $-88^{\circ}\text{C}$  (Brunner et al., 2008).

Encounters with cirrus clouds have been selected from the dataset. A cirrus encounter was defined as a time period of at least 30 s in which particles with sizes beyond the lower detection limit of the FSSP-100 ( $2.7\ \mu\text{m}$  diameter) were detected at temperatures below  $-35^{\circ}\text{C}$ . When the aircraft changed altitude, the averaging times were chosen in a way that the altitude over which was averaged was not larger than 1 km. Moreover, for longer encounters with cirrus clouds, more averages were made, so that the maximum averaging time was 430 s. In total 90 cirrus encounters, between 10 and 19 km altitude, were selected with an average duration of 138 s (corresponding to a horizontal distance of about 26 km).

For each cirrus encounter the ice crystal size distribution has been calculated by

Title Page

Abstract

Introduction

Conclusions

References

Tables

Figures

◀

▶

◀

▶

Back

Close

Full Screen / Esc

Printer-friendly Version

Interactive Discussion



combining the data of the FSSP and CIP. To put the observed ice crystal size distribution data in an atmospheric perspective, other parameters (e.g. temperature, pressure, altitude) have been averaged over the same time period.

### 3.1 Ice crystal size distributions

5 The ice crystal size distributions (normalised to a total  $dN/d\log D_p$  value of 1) of the 90 cirrus encounters are presented in Fig. 2 in potential temperature bins of 10 to 20 degrees. Ice crystals observed at potential temperatures exceeding 385 K are clearly situated in the stratosphere. The region between 365 and 385 K is influenced by tropospheric and stratospheric airmasses and is referred to as the tropopause region, while  
10 airmasses below 365 K are clearly tropospheric. From Fig. 2 it is unambiguous that ice crystals have been observed in the stratosphere. The five stratospheric size distributions shown in the upper panel of Fig. 2 are all observed during the first flight on 30 November when the Geophysica aircraft encountered an area with ice crystals in the tropical stratosphere directly over the Hector convective system. A detailed discussion  
15 about these stratospheric ice crystals and its origin can be found in Sect. 3.3.

The majority of the ice crystal number size distributions peaks between 6 and 15  $\mu\text{m}$  diameter. Only 7% of the distributions show a monotonically decreasing distribution with size, with a maximum number concentration at sizes below 3  $\mu\text{m}$  diameter, which could be due to the more recent formation of small ice crystals (Schröder et al., 2000) or sublimation of larger ice crystals. Since we have no additional information about the  
20 age of the different ice clouds, this has not been studied in detail. From Fig. 2 it can also be seen that the largest particles, up to 1 mm maximum dimension, are observed in the lowest potential temperature bin. While ascending to the tropopause region the size of the largest observed ice crystal decreases. Larger particles, with a maximum  
25 dimension up to 400  $\mu\text{m}$ , are observed again in the stratosphere.

In order to learn about the shape of the size distribution two/three modal lognormal size distributions were fitted to the median normalised size distribution in each potential temperature bin (red lines in Fig. 2). The number concentration, mean mode diameter

## Ice particles in the tropical stratosphere

M. de Reus et al.

Title Page

Abstract

Introduction

Conclusions

References

Tables

Figures

◀

▶

◀

▶

Back

Close

Full Screen / Esc

Printer-friendly Version

Interactive Discussion



**Ice particles in the tropical stratosphere**

M. de Reus et al.

Title Page

Abstract

Introduction

Conclusions

References

Tables

Figures

◀

▶

◀

▶

Back

Close

Full Screen / Esc

Printer-friendly Version

Interactive Discussion



and standard deviation of each mode describing the lognormal distribution are given in Table 1. When ascending from the lowest level in the troposphere to the tropopause region, the mean mode diameter of the smallest modes shifts to smaller sizes and the largest mode even disappears in the upper troposphere and tropopause region. For example the mean mode diameter of the second mode decreases from 35  $\mu\text{m}$  in the middle troposphere to 25  $\mu\text{m}$  in the upper troposphere, and 18  $\mu\text{m}$  in the tropopause region. The size distributions observed in the stratosphere, however, do not follow this trend, but are similar to the ones observed in the upper troposphere.

Figure 2 also includes normalised ice crystal size distributions calculated according to the parameterisation reported by McFarquhar and Heymsfield (1997). The average ice water content and ambient temperature which have been observed within the potential temperature bins are taken as input for these calculations. The size distributions calculated according to the parameterisation show a similar decrease in ice crystal size with increasing potential temperature in the troposphere, but generally a more pronounced mode at diameters exceeding 100  $\mu\text{m}$  is found. Due to the higher ambient temperature in the stratosphere compared to the tropopause region, the largest mode which is absent in the tropopause region appears again higher up in the stratosphere, as has been observed in this study. We have to note however, that the parameterisation is based on size distribution measurements inside tropical cirrus clouds at temperatures down to  $-70^{\circ}\text{C}$ , while the ambient temperatures in this study were  $-53$ ,  $-80$ ,  $-86$ , and  $-83^{\circ}\text{C}$  for the bottom to the top panel, respectively. A discussion about other reported size distribution can be found below.

A two-modal ice crystal size distribution for crystals smaller than 60  $\mu\text{m}$  diameter has also been retrieved from satellite measurements in a cirrus cloud associated with a tropical convective system (Eremenko et al., 2005). These measurements show a bimodal size distribution with a pronounced second mode at altitudes exceeding 15 km. The smaller mode peaks at about 6  $\mu\text{m}$  diameter and the larger mode at 20–40  $\mu\text{m}$  diameter, comparable to the distributions shown in this study. The existence of a third mode could not be confirmed due to the fact that only particles with diameters  $<60 \mu\text{m}$

**Ice particles in the  
tropical stratosphere**

M. de Reus et al.

[Title Page](#)[Abstract](#)[Introduction](#)[Conclusions](#)[References](#)[Tables](#)[Figures](#)[◀](#)[▶](#)[◀](#)[▶](#)[Back](#)[Close](#)[Full Screen / Esc](#)[Printer-friendly Version](#)[Interactive Discussion](#)

diameter can be retrieved from this satellite measurement. Model calculations for a precipitating anvil show a tri-modal cloud particle size distribution. The smallest particles, with a modal value around  $10\ \mu\text{m}$  diameter, originate mainly from frozen interstitial haze drops, which normally do not freeze until the temperature decreases below  $-40^\circ\text{C}$ , the medium sized particles ( $100\ \mu\text{m}$ ) are mainly from frozen cloud drops and the largest particles ( $1\ \text{mm}$ ) mainly from crystal aggregates and rimed ice (Chen et al., 1997). This larger mode has not been observed in our measurements since the ice crystal size distributions presented in this study are mainly observed in the (detached) anvil of the Hector convective system and not directly in the Hector system itself where precipitation could occur.

### 3.2 Effective radius and ice water content

From the observed size distributions several parameters have been deduced, among them the effective radius, the ice crystal number concentration and the ice water content, which are shown in Fig. 3 as a function of the potential temperature.

The effective radius (defined as the ratio of the third to the second moment of a size distribution, in terms of spheres of equivalent cross-section area (McFarquar and Heymsfield, 1998)) is one of the key variables that are used for the calculation of the radiative properties of clouds, since it is proportional to the ratio of the ice water content and the extinction coefficient (Heymsfield et al., 2006). For the selected cirrus events the effective radius ranges from  $3$  to  $100\ \mu\text{m}$  and decreases with increasing potential temperature (and altitude and ambient temperature). This is in agreement with observations and model calculations in the tropics presented by Chen et al. (1997), who show a decreasing effective radius with altitude. Also Garrett et al. (2003) observed a decreasing effective radius with ambient temperature in the sub-tropics. They suggest that this is caused by the fact that homogeneous ice nucleation favours smaller ice crystals at colder temperatures, due to the exponential dependence of the saturation vapour pressure over ice on temperature (Kärcher and Lohmann, 2002), rather than the effect of aging of the cirrus cloud or gravitational settling.

**Ice particles in the  
tropical stratosphere**

M. de Reus et al.

[Title Page](#)[Abstract](#)[Introduction](#)[Conclusions](#)[References](#)[Tables](#)[Figures](#)[I◀](#)[▶I](#)[◀](#)[▶](#)[Back](#)[Close](#)[Full Screen / Esc](#)[Printer-friendly Version](#)[Interactive Discussion](#)

The observed total ice crystal number concentration was low. Within the cirrus clouds it ranged between 0.01 and 0.7 cm<sup>-3</sup> and shows no clear correlation with potential temperature, although the highest ice crystal number concentrations are found at lower altitudes. Note here that for the thin and patchy cirrus clouds observed in this study the ice crystal number concentration depends very much on the position within the cloud and the chosen averaging times.

The ice water content has been calculated from the observed ice crystal size distribution using the algorithm proposed by Brown and Francis (1995). They use the relation between mass ( $M$  in g) and ice crystal maximum dimension ( $D$  in  $\mu\text{m}$ ) of Locatelli and Hobbs (1974):  $M = aD^b$ . For ice crystals with a size larger than 100  $\mu\text{m}$  they determined  $a = 7.38 \times 10^{-11}$  and  $b = 1.9$ , smaller ice crystals are assumed to be solid ice spheres with a density of 0.917 g cm<sup>-3</sup>. The uncertainty in the resulting IWC has been estimated to be a factor 2 (Heymsfield, 2007).

Following the fact that smaller particles are observed with increasing potential temperature, the IWC is found to decrease with increasing potential temperature. A gradual decrease in ice water content with ambient temperature has also been observed by McFarquhar and Heymsfield (1997) in a tropical area at temperatures between  $-20^\circ\text{C}$  and  $-70^\circ\text{C}$ , and by Schiller et al. (2008) for a dataset containing polar, mid-latitude and tropical cirrus clouds at temperatures ranging from  $-23^\circ\text{C}$  to  $-90^\circ\text{C}$ . Note that the observed IWC is much lower as the IWC reported by Knollenberg et al. (1993) over the same area and corresponding altitudes during the STEP Tropical Experiment at Darwin in January/February 1987.

The ice water content calculated from the ice crystal size distributions has been compared with the ice water content determined from the two hygrometer (FISH and FLASH) measurements and is shown in Fig. 4. The total uncertainty in the derivation of the IWC from the two hygrometer instruments is dependent on the exact position of the inlets of the hygrometers, the calculated enhancement factor of the FISH and the measurement uncertainty of the individual instruments and is estimated to be 20%. For the IWC intercomparison hygrometer data for the flights on 29 and 30 November

(double flight) are used, which are also included in the evaluation of the ice water content in Arctic, mid-latitude and tropical cirrus reported by Schiller et al. (2008).

The IWC derived using these two very different methods shows a close correlation, however, not on the 1:1 line. In airmasses with a low IWC the hygrometer data shows higher values than the IWC calculated from the ice crystal size distributions. At higher IWC, the two measurements seem to agree much better. Considering the entire dataset shown in Fig. 4, 90% of the data points lie within a factor four of the 1:1 line. For ice water contents exceeding  $2 \times 10^{-4} \text{ g m}^{-3}$  the IWC determined by the two very different measurement methods agree within the combined uncertainty of the instruments (i.e. factor 2.2, see thin solid lines in Fig. 4). At low IWC, the ice crystal size distribution mainly consists of small particles, so that the FSSP size range contributes more than 75% to the observed IWC (red markers in Fig. 4). Here, the IWC is underestimated by the microphysical measurements, indicating that shattering is not a problem for the microphysical probes at these low IWCs, since in case of shattering the IWC should be overestimated. However, note that at very low IWC the uncertainty in both methods might be higher as indicated above, since at the lowest observed IWC the total water content measured by the FISH instrument is not more than a factor two higher than the water vapour concentration measured by the FLASH. Moreover, for the IWC derivation from the ice crystal size distribution in Brown and Francis (1995) the IWC ranged from 0.001 to  $0.5 \text{ g m}^{-3}$ , and shows large scatter for IWC below  $0.01 \text{ g m}^{-3}$ .

We investigated if an erroneous calculation of the IWC from the size distribution measurements ( $\text{IWC} = a \times D^b$ ) could have caused the difference in IWC derived via the two different methods. However, no realistic combination of the  $a$  and  $b$  factor can be found which brings all data points within the combined uncertainty of both methods (thin solid lines in Fig. 4). When we reduce “ $b$ ” to 1.7, the agreement between both methods improves at high IWC. However, this does not change the underestimation of the IWC calculation from the size distribution at lower IWC, since this is determined by smaller particles which are assumed to be solid spheres. Here only an underestimation of the ice crystal number concentration, measured by the FSSP can explain the low IWC

## Ice particles in the tropical stratosphere

M. de Reus et al.

Title Page

Abstract

Introduction

Conclusions

References

Tables

Figures

◀

▶

◀

▶

Back

Close

Full Screen / Esc

Printer-friendly Version

Interactive Discussion



values derived from the ice crystal size distribution measurements.

### 3.3 Ice crystals in the stratosphere

On 30 November 2005 a flight was performed to investigate the Hector convective system. The flight track of this flight is shown in Fig. 5. A large part of the flight was conducted in the stratosphere above the Hector system. While looking for outflow regions, the aircraft curved above the Hector system and, according to the pilot's report, succeeded to pass through a visible hazy area twice. From the FSSP data six time periods could be selected during which ice crystals were observed for at least 30 s. Unfortunately, CIP data during one time period (No. 5) was lost. The ice crystal size distributions of the five remaining time periods are shown in Fig. 2 (top panel), while the parameters characterising the ice crystal size distribution and the meteorological situation are summarised in Table 2. Moreover, in Fig. 6a the time series of temperature, altitude, ice crystal number concentration, relative humidity, ozone mixing ratio and total water content for the stratospheric part of the flight on 30 November 2005 are shown. In this figure the selected time periods are shaded and the events are numbered.

Finally Fig. 6b shows the vertical profile of aerosol and cloud particles below the aircraft, as observed by a downward looking Miniature Aerosol Lidar (MAL), which allows observations as close as 160 m from the aircraft (Mitev et al., 2002).

The ice crystals were observed at altitudes between 18 and 18.7 km, at temperatures between  $-81$  to  $-87^{\circ}\text{C}$  and pressures ranging from 68 to 78 hPa, which corresponds to a potential temperature level between 386 and 414 K. The cold point tropopause was situated at 17.3 km altitude during this day, hence, the ice crystals were observed between 0.7 to 1.4 km above the tropopause. During four events the air was subsaturated with respect to ice (RH<sub>i</sub> varied between 75 and 95%) indicating a cloud in its decaying state. The remaining two time period (2 and 4) show a supersaturation, with an average relative humidity over ice of 107% and 157%, respectively, which indicates either recent ice crystal formation or recent updraft from the troposphere. The ice

## Ice particles in the tropical stratosphere

M. de Reus et al.

Title Page

Abstract

Introduction

Conclusions

References

Tables

Figures

◀

▶

◀

▶

Back

Close

Full Screen / Esc

Printer-friendly Version

Interactive Discussion



**Ice particles in the  
tropical stratosphere**

M. de Reus et al.

[Title Page](#)[Abstract](#)[Introduction](#)[Conclusions](#)[References](#)[Tables](#)[Figures](#)[◀](#)[▶](#)[◀](#)[▶](#)[Back](#)[Close](#)[Full Screen / Esc](#)[Printer-friendly Version](#)[Interactive Discussion](#)

crystal size distribution can be characterised by the effective radius ( $R_{\text{eff}}$ ), an area weighted mean radius of the ice crystals, or by the geometric mean radius ( $R_{\text{mean}}$ ), which is a number weighted mean radius of the ice crystals. During the five selected time periods,  $R_{\text{eff}}$  ranged between 12 and 25  $\mu\text{m}$  and  $R_{\text{mean}}$  between 4.6 and 9.3  $\mu\text{m}$ .

5 The ice water content calculated from the observed ice crystal size distribution varied between  $8.4 \times 10^{-5}$  and  $1.7 \times 10^{-3} \text{ g m}^{-3}$ , and was within a factor two from the IWC derived from the two hygrometers. Note that the observed IWCs are larger by several orders of magnitude than those of the climatology at these low temperatures (Schiller et al., 2008)

10 From Fig. 6a it can be seen that, except for event 1, the increase in ice crystal number concentration corresponds with a decrease in  $\text{O}_3$  mixing ratio and temperature, which is indicative for updraft of tropospheric air into the stratosphere. Hence, the ice crystals in the stratosphere result from overshooting convection of the Hector system. This is supported by the backscatter ratio profiles measured by the lidar, which show the convective system below the aircraft, reaching down to the local tropopause.

15 Event 1 does not show a clear tropospheric signature, which might be a result of mixing of tropospheric and stratospheric air. Another possible explanation for the missing tropospheric signature in this airmass is that the ice crystals are formed in-situ in the stratosphere (pileus cloud). This can be excluded, because the observed ice crystals are much too large to be formed in-situ. Garrett et al. (2006), for example, show a pileus cloud with effective radii between 2 and 4  $\mu\text{m}$ . However, also during this time period the lidar shows ice crystals down to the local tropopause, indicating overshooting convection as source for the ice crystals.

25 The terminal settling velocity (calculated after Mitchell and Heymsfield, 2005) of the ice crystals observed in the stratosphere has been calculated in order to determine its potential residence time in the stratosphere and thereby its potential for humidifying the stratosphere. Note that for these calculations the size of the ice crystals is kept constant, the reduction in size of the ice crystals by sublimation has not been taken into account. Figure 7 shows the settling velocity for the ice crystal sizes observed

**Ice particles in the tropical stratosphere**

M. de Reus et al.

Title Page

Abstract

Introduction

Conclusions

References

Tables

Figures

◀

▶

◀

▶

Back

Close

Full Screen / Esc

Printer-friendly Version

Interactive Discussion



during event 1 in Fig. 6, since during this event the largest crystals were observed in the stratosphere. The settling velocity ranges from  $0.001 \text{ cm s}^{-1}$  for ice crystals with a size of  $3.7 \mu\text{m}$  to  $54 \text{ cm s}^{-1}$  for  $438 \mu\text{m}$  sized particles. Subsequently, the stratospheric residence time, based on gravitational settling only, has been calculated using the height above the tropopause, where the ice crystals were observed, as travelling distance. During the first event, where the ice crystals were observed  $0.7 \text{ km}$  above the tropopause, the residence time ranges from  $0.5 \text{ hour}$  to many days. The black lines in Fig. 7 indicate that ice crystals with sizes larger than about  $100 \mu\text{m}$  will be removed from the stratosphere within one hour, while particles smaller than  $40 \mu\text{m}$  will remain in the stratosphere for more than a day. Ice crystals have been observed up to  $1.4 \text{ km}$  above the troposphere, which means that even the largest observed ice crystal would stay in the stratosphere for over one hour, and potentially hydrate the stratosphere. Detailed model calculations including sublimation and mixing processes have to be performed to determine how much water vapour will remain in the stratosphere.

### 3.4 Interstitial aerosols

The aerosol number concentration measured with the COPAS instrument during the five investigated flights are shown in Fig. 8. The number concentration of interstitial aerosol (non-activated particles in between the ice crystals) is shown as coloured dots, while the particle concentrations measured in clear air masses (no ice crystals observed) are shown as grey dots. The large markers show the average interstitial aerosol concentration within the selected ice clouds.

The total aerosol number concentration ( $N_{14}$ ) decreases with increasing potential temperature from about  $200 \text{ cm}^{-3}$  at  $355 \text{ K}$  to less than  $20 \text{ cm}^{-3}$  at  $435 \text{ K}$ . At the same time, the number concentration of non volatile aerosols ( $N_{10\text{nv}}$ ) decreases from  $100 \text{ cm}^{-3}$  to  $10 \text{ cm}^{-3}$ . Since no information about the aerosol number concentration in the boundary layer is available, no statement can be made about possible enhanced particle concentrations in the outflow region of convective clouds, as has been ob-

served by de Reus et al. (2001) over the northern Indian Ocean.

Ultrafine particles ( $N_{6-14}$ ) are mainly observed in the troposphere, with concentrations ranging from 10 to more than  $1000\text{ cm}^{-3}$ . Particles in this size range must have been formed by nucleation processes in the atmosphere, because particles from primary sources are always larger in size. Therefore, it is very unlikely that these particles are transported from the boundary layer within the Hector convective system. Furthermore, their formation must have been recent because nucleation mode particles exist typically only for a few hours to one day since the aerosols grow by condensation and are lost by coagulation with larger particles (Curtius, 2006). Therefore, we presume that the ultrafine particles have been formed in the outflow of the Hector storm system. This region is favourable for new particle formation due to the relatively high precursor gas concentrations transported from the lower troposphere, a low pre-existing particle surface area due to the scavenging of large particles in the cloud and the low ambient temperature in the outflow region (de Reus et al., 2001).

The vertical profile of the aerosol number concentration in and out of clouds do not differ much in the troposphere. Within the stratospheric ice clouds ( $>385\text{ K}$ ), however, the total as well as the non-volatile aerosol number concentration is enhanced compared to the out-of-cloud concentrations, supporting the hypothesis that these air masses are transported from the troposphere by overshooting convection. The presence of ultrafine particles in the stratospheric ice clouds might indicate recent new particle formation, although the observed number concentrations are low compared to earlier observations of new particle formation in tropical cirrus clouds (Lee et al., 2004).

In Fig. 9 the relation between the interstitial particle number concentration and ice crystals number concentration is shown. The idea behind this plot was to find out how many aerosol particles out of the measured total number of available particles would end up as cloud ice particles. As the three lines show the ratio between interstitial aerosols and ice crystals ranges from 1:300 to 1:30 000. To show that this range of ratios is also observed during other campaigns in the tropics, data collected during the AMMA campaign (Burkina Faso, August 2006) using the same instrumentation and

## Ice particles in the tropical stratosphere

M. de Reus et al.

Title Page

Abstract

Introduction

Conclusions

References

Tables

Figures

◀

▶

◀

▶

Back

Close

Full Screen / Esc

Printer-friendly Version

Interactive Discussion



research aircraft are also included.

Seifert et al. (2004) investigated the relation between the interstitial particle number concentration and the ice crystal number concentration for mid-latitude cirrus clouds in the northern and southern hemisphere. They found that the number concentration of interstitial aerosols and ice crystals were positively related at low interstitial number concentrations ( $<100 \text{ cm}^{-3}$ ) and negatively correlated at higher aerosol concentrations. They explained this behaviour by different phases of the cirrus lifecycle. Cloud formation is associated with positive correlations, while the correlations are smaller or even negative in dissolving clouds. Although this theory cannot directly be translated to the SCOUT data in Fig. 9, since here averages of cloud events are shown and not the correlation within a single cirrus cloud, this work suggests that the ratio is very dependent on the development stage of the cloud.

## 4 Discussion

### 4.1 Spatial extend of overshooting convection

The effect of overshooting convection on the global stratospheric water budget is dependent on the frequency and the spatial scale of overshooting events. From the one event discussed in this paper it is impossible to make any statements about the frequency and average spatial scale of an overshooting event. That overshooting happens more regularly is shown by Corti et al. (2008), who report on overshooting convection events during 6 out of 16 flights in the tropical stratosphere over Australia and the South American continent. However, it should be noted that the flight strategy during these campaigns was very much focussed on the investigation of potential overshoots.

Figure 5 shows the flight track of the discussed flight and the encounters with ice crystals in the stratosphere. The horizontal extend of the ice cloud is 0.27 degrees latitude and 0.36 longitude, corresponding to about  $30 \text{ km} \times 40 \text{ km}$ . Ice crystals were observed between 0.7 and 1.4 km above the tropopause, but not at 1.5 km above the

## Ice particles in the tropical stratosphere

M. de Reus et al.

Title Page

Abstract

Introduction

Conclusions

References

Tables

Figures



Back

Close

Full Screen / Esc

Printer-friendly Version

Interactive Discussion



tropical tropopause. At times between the different encounters with the ice crystals, measurements at the same geographical position at 18.8 km altitude show that no ice particles were present at this altitude. Moreover, lidar measurements indicate that the ice crystals were observed down to the local tropopause (Fig. 6b). Hence, the spatial scale of this overshooting event is about  $30 \times 40 \times 1.4$  km. Note, however, that the “cloud” structure is patchy, and not completely filled with ice crystals.

## 4.2 Potential artefacts by shattering

Ice crystal size distribution and number concentration measurements by microphysical probes as the FSSP and CIP are currently the subject of intensive discussions, due to its potential shattering problem (Field et al., 2006; McFarquar et al., 2007; Heymsfield, 2007). Due to the high airspeed of the aircraft used for in-situ measurements, ice particles several hundred microns or larger can hit the forward surfaces of the probes, shatter and produce a large number of small particles. This causes an overestimation of the number concentration of small particle number concentration observed by for example the FSSP probe. The CIP data have been corrected for potential shattering events using the interarrival time method proposed by Field et al. (2006). This method assumes that shattering of a large ice crystal causes a burst of small particles with very short interarrival times, which can be distinguished from the longer interarrival times of real cloud particles in a cirrus cloud (see Fig. 1b). Since information about the interarrival time of crystals observed by the FSSP probe is not available we have investigated the shattering problem for our data set by comparing it to a data set which is not influenced by shattering as proposed by Heymsfield (2007). This data set, presented by McFarquar and Heymsfield (1997), has been the basis for a parameterisation for cirrus cloud size distributions using the temperature and total ice water content as input value. Using the observed IWC and temperature we calculated the IWC for the size ranges of the FSSP and CIP and compared this to the IWC measured by the two individual instruments (see Fig. 10). At low IWC both datasets show a similar distribution of the ice water content between the two observed size ranges, while at higher IWC the IWC

## Ice particles in the tropical stratosphere

M. de Reus et al.

Title Page

Abstract

Introduction

Conclusions

References

Tables

Figures

◀

▶

◀

▶

Back

Close

Full Screen / Esc

Printer-friendly Version

Interactive Discussion



measured by the FSSP is below the predicted value by the MH97 parameterisation. When shattering occurs the IWC for the FSSP size range should be overestimated, as has been shown by Heymsfield (2007). Despite the low ice water content measured by the FSSP, the linear relation between the  $IWC_{FSSP}$  and the  $IWC_{CIP}$  at higher IWC ( $>10^{-4} \text{ g m}^{-3}$ ) might be an indication for the occurrence of shattering. To summarise, our dataset shows no indication for a severe shattering problem for  $IWC < 10^{-4} \text{ g m}^{-3}$ . At higher IWC we cannot exclude the occurrence of shattering.

## 5 Summary and conclusions

Ice crystals with sizes up to  $400 \mu\text{m}$  have been observed in the tropical stratosphere, up to 1.4 km above the local tropopause, directly above the Hector storm system. These particles have been transported into the stratosphere by overshooting convection and are remnants of a very fresh overshooting top. Ice crystals have been observed in an area of about  $30 \times 40 \text{ km}$  and might be very important for humidifying the stratosphere.

In the tropical troposphere a decrease in effective radius was observed with altitude (or potential temperature), which could also be represented by three modal lognormal size distributions fitted to the average observed size distribution at different potential temperature levels. The lognormal distributions show a decrease in mean mode diameter of all three modes when ascending towards the tropopause. The ice water content decreases accordingly.

*Acknowledgements.* We thank Sebastian Raupach, Christian von Glahn and Hermann Vössing from the University of Mainz for carrying out the CIP and FSSP instrument preparation and data collection during the SCOUT- $\text{O}_3$  campaign. The SCOUT- $\text{O}_3$  project was funded by the European Commission (GOCE-CT-2004-505390). Financial support by the Max Planck Society and the Collaborative Research Centre “The Tropospheric Ice Phase” (SFB-641) is also gratefully acknowledged. The participation of Aaron Bansemer and Andrew Heymsfield to the SCOUT/ACTIVE project was funded by the University of Manchester. Special thanks to the entire Geophysica crew and the local authorities in Darwin (Australia) and Ouagadougou

Title Page

Abstract

Introduction

Conclusions

References

Tables

Figures

◀

▶

◀

▶

Back

Close

Full Screen / Esc

Printer-friendly Version

Interactive Discussion



(Burkina Faso) for their excellent collaboration during the campaign. Many helpful comments from the participants of the Oral Session 5 on Cirrus Clouds during the 15th International Conference on Clouds and Precipitation, July 2008 in Cancun, Mexico are greatly appreciated.



This Open Access Publication is  
financed by the Max Planck Society.

5 MAX-PLANCK-GESELLSCHAFT

## References

- 10 Baumgardner, D., Dye, J. E., Gandrud, B. W., and Knollenberg, R. G.: Interpretation of measurements made by the forward scattering spectrometer probe (FSSP-300) during the airborne arctic stratospheric expedition, *J. Geophys. Res.*, 97, 8035–8046, 1992.
- Baumgardner, D. and Korolev, A.: Airspeed corrections for optical array probe sample volumes, *J. Atmos. Oceanic Technol.*, 14, 1224–1229, 1997.
- 15 Borrmann, S., Solomon, S., Dye, J. E., and Luo, B.: The potential of cirrus clouds for heterogeneous chlorine activation, *Geophys. Res. Lett.*, 23, 2133–2136, 1996.
- Borrmann, S., Luo, B., and Mishchenko, M.: The application of the T-matrix method to the measurement of aspherical particles with forward scattering optical particle counters, *J. Aerosol Sci.*, 31, 789–799, 2000.
- 20 Brown, P. R. A. and Francis, P. N.: Improved measurements of the ice water content in cirrus using a total water probe, *J. Atmos. Oceanic Technol.*, 12, 410–414, 1995.
- Brunner, D., Siegmund, P., May, P. T., Chappel, L., Schiller, C., Müller, R., Peter, T., Fueglistaler, S., MacKenzie, A. R., Fix, A., Schlager, H., Allen, G., Fjaeraa, A. M., Streibel, M., and Harris, N. R. P.: The SCOUT-O3 Darwin Aircraft Campaign: rationale and meteorology, *Atmos. Chem. Phys. Discuss.*, 8, 17 131–17 191, 2008, <http://www.atmos-chem-phys-discuss.net/8/17131/2008/>.
- 25 Chaboureaud, J.-P., Cammas, J.-P., Duron, J., Mascart, P. J., Sitnikov, N. M., and Voessing, H.-J.: A numerical study of tropical cross-tropopause transport by convective overshoots,

ACPD

8, 19313–19355, 2008

## Ice particles in the tropical stratosphere

M. de Reus et al.

Title Page

Abstract

Introduction

Conclusions

References

Tables

Figures

◀

▶

◀

▶

Back

Close

Full Screen / Esc

Printer-friendly Version

Interactive Discussion



Atmos. Chem. Phys., 7, 1731–1740, 2007,  
<http://www.atmos-chem-phys.net/7/1731/2007/>.

Chen, J. P., McFarquhar, G. M., Heymsfield, A. J., and Ramanathan, V.: A modelling and observational study of the detailed microphysical structure of tropical cirrus anvils, *J. Geophys. Res.*, 102, 6637–6653, 1997.

Connolly, P. J., Choulaton, T. W., Gallagher, M. W., Bower, K. N., Flynn, M. J., and Whiteway, J. A.: Cloud-resolving simulations of intense tropical Hector thunderstorms: Implications for aerosol-cloud interactions, *Q. J. Roy. Meteorol. Soc.*, 132, 3079–3106, 2006.

Corti, T., Luo, B. P., de Reus, M., Brunner, D., Cairo, F., Mahoney, M. J., Martucci, G., Matthey, R., Mitev, V., dos Santos, F. H., Schiller, C., Shur, G., Sitnikov, N. M., Spelten, N., Vössing, H. J., Borrmann, S., and Peter, T.: Unprecedented evidence for overshooting convection hydrating the tropical stratosphere, *Geophys. Res. Lett.*, 35, L10810, doi:10.1029/2008GL033641, 2008.

Curtius, J., Weigel, R., Vössing, H.-J., Wernli, H., Werner, A., Volk, C.-M., Konopka, P., Kreischbach, M., Schiller, C., Roiger, A., Schlager, H., Dreiling, V., and Borrmann, S.: Observations of meteoric material and implications for aerosol nucleation in the winter Arctic lower stratosphere derived from in situ particle measurements, *Atmos. Chem. Phys.*, 5, 3053–3069, 2005,  
<http://www.atmos-chem-phys.net/5/3053/2005/>.

Curtius, J.: Nucleation of atmospheric aerosol particles, *C. R. Physique*, 7, 1027–1045, 2006.  
de Reus, M., Krejci, R., Williams, J., Fischer, H., Scheele, R., and Ström, J.: Vertical and horizontal distributions of the aerosol number concentration and size distribution over the northern Indian Ocean, *J. Geophys. Res.*, 106, 28 629–28 641, 2001.

Dye, J. E. and Baumgardner, D.: Evaluation of the Forward Scattering Spectrometer Probe. Part I: Electronic and optical studies, *J. Atmos. Oceanic Technol.*, 1, 329–344, 1984.

Eremenko, M. N., Zasetsky, A. Y., Boone, C. D., and Sloan, J. J.: Properties of high-altitude tropical cirrus clouds determined from ACE FTS observations, *Geophys. Res. Lett.*, 32, 15S07, doi:10.1029/2005GL022428, 2005.

Field, P. R., Heymsfield, A. J., and Bansemer, A.: Shattering and particle interarrival times measured by optical array probes in ice clouds, *J. Atmos. Oceanic Technol.*, 23, 1357–1371, 2006.

Garrett, T. J., Gerber, H., Baumgardner, D. G., Twohy, C. H., and Weinstock, E. M.: Small, highly reflective ice crystals in low-latitude cirrus, *Geophys. Res. Lett.*, 30, 2132,

ACPD

8, 19313–19355, 2008

## Ice particles in the tropical stratosphere

M. de Reus et al.

Title Page

Abstract

Introduction

Conclusions

References

Tables

Figures

◀

▶

◀

▶

Back

Close

Full Screen / Esc

Printer-friendly Version

Interactive Discussion



doi:10.1029/2003GL018153, 2003.

Garrett, T. J., Dean-Day, J., Liu, C., Barnett, B., Mace, G., Baumgardner, D., Webster, C., Bui, T., Read, W., and Minnis, P.: Convective formation of pileus cloud near the tropopause, *Atmos. Chem. Phys.*, 6, 1185–1200, 2006,

<http://www.atmos-chem-phys.net/6/1185/2006/>.

Gayet, J. F., Ovarlez, J., Shcherbakov, V., Ström, J., Schumann, U., Minikin, A., Auriol, F., Petzold, A., and Monier, M.: Cirrus cloud microphysical and optical properties at southern and northern midlatitudes during the INCA Experiment, *J. Geophys. Res.*, 109, D20206, doi:10.1029/2004JD004803, 2004.

Heymsfield, A. J. and Parrish, J. L.: A computational technique for increasing the effective sampling volume of the PMS two-dimensional particle size spectrometer, *J. Appl. Meteor.*, 17, 1566–1572, 1978.

Heymsfield, A. J.: Ice particles observed in a cirriform cloud at  $-83^{\circ}\text{C}$  and implications for polar stratospheric clouds, *J. Atmos. Sci.*, 43, 851–855, 1986.

Heymsfield, A. J. and McFarquhar, G. M.: Midlatitude and tropical cirrus – microphysical properties, in *Cirrus*, edited by: Lynch, D. K., Sassen, K., Starr, D. O., and Stephens, G., Oxford Univ. Press, New York, 2002.

Heymsfield, A. J., Schmidt, C., Bansemer, A., van Zadelhoff, G. J., McGill, M. J., Twohy, C., and Baumgardner, D.: Effective radius of ice cloud particle populations derived from aircraft probes, *J. Atmos. Oceanic Technol.*, 23, 361–380, 2006.

Heymsfield, A. J.: On measurements of small ice particles in clouds, *Geophys. Res. Lett.*, 34, L23812, doi:10.1029/2007GL030951, 2007.

Kärcher, B. and Lohmann, U.: A parameterization of cirrus cloud formation: Homogeneous freezing of supercooled aerosols, *J. Geophys. Res.*, 107, 4010, doi:10.1029/2001JD000470, 2002.

Knollenberg, R. G.: The optical array: an alternative to scattering or extinction for airborne particle size determination, *J. Appl. Meteor.*, 9, 86–103, 1970.

Knollenberg, R. G., Kelly, K., and Wilson, J. C.: Measurements of high number densities of ice crystals in the tops of tropical cumulonimbus, *J. Geophys. Res.*, 98, 8639–8664, 1993.

Korolev, A. V., Strapp, J. W., and Isaac, G. A.: Evaluation of the accuracy of PMS Optical Array Probes, *J. Atmos. Oceanic Technol.*, 15, 708–720, 1998.

Lee, S. H., Wilson, J. C., Baumgardner, D., Herman, R. L., Weinstock, E. M., LaFleur, B. G., Kok, G., Anderson, B., Lawson, P., Baker, B., Strawa, A., Pittman, J. V., Reeves, J. M.,

Ice particles in the tropical stratosphere

M. de Reus et al.

Title Page

Abstract

Introduction

Conclusions

References

Tables

Figures

◀

▶

◀

▶

Back

Close

Full Screen / Esc

Printer-friendly Version

Interactive Discussion



**Ice particles in the  
tropical stratosphere**

M. de Reus et al.

Title Page

Abstract

Introduction

Conclusions

References

Tables

Figures

◀

▶

◀

▶

Back

Close

Full Screen / Esc

Printer-friendly Version

Interactive Discussion



- and Bui, T. P.: New particle formation observed in the tropical/subtropical cirrus clouds, *J. Geophys. Res.*, 109, D20209, doi:10.1029/2004JD005033, 2004.
- Locatelli, J. D. and Hobbs, P. V.: Fall speeds and masses of solid precipitation particles, *J. Geophys. Res.*, 79, 2185–2197, 1974.
- 5 Lynch, D. K., Sassen, K., Starr, D. O., and Stephens, G. (Eds.): *Cirrus*, Oxford Univ. Press, New York, 2002.
- McFarquhar, G. M. and Heymsfield, A. J.: Parameterisation of tropical cirrus ice crystal size distributions and implications for radiative transfer: results from CEPEX, *J. Atmos. Sci.*, 54, 2187–2200, 1997.
- 10 McFarquhar, G. M. and Heymsfield, A. J.: The definition and significance of an effective radius for ice clouds, *J. Atmos. Sci.*, 55, 2039–2052, 1998.
- McFarquhar, G. M., Heymsfield, A. J., Spinhirne, J., and Hart, B.: Thin and subvisual tropopause tropical cirrus: observations and radiative impacts, *J. Atmos. Sci.*, 57, 1841–1853, 2000.
- 15 McFarquhar, G. M., Um, J., Freer, M., Baumgardner, D., Kok, G. L., and Mace, G.: Importance of small ice crystals to cirrus properties: Observations from the tropical warm pool international cloud experiment (TWP-ICE), *Geophys. Res. Lett.*, 34, L13803, doi:10.1029/2007GL029865, 2007.
- Mitchell, D. L. and Heymsfield, A. J.: Refinements in the Treatment of ice particle terminal velocities, highlighting aggregates, *J. Atmos. Sci.*, 62, 1637–1644, 2005.
- Mitev, V., Matthey, R., and Makanov, V.: Miniature backscatter lidar for cloud and aerosol observation from high altitude aircraft, *Recent Res. Dev. Geophys.*, 4, 207–223, 2002.
- Nielsen, J. K., Larsen, N., Cairo, F., Di Donfrancesco, G., Rosen, J. M., Durrý, G., Held, G., and Pommereau, J. P.: Solid particles in the tropical lowest stratosphere, *Atmos. Chem. Phys.*, 7, 685–695, 2007,
- 25 <http://www.atmos-chem-phys.net/7/685/2007/>.
- Oltmans, S. J., Vömel, H., Hofmann, D. J., Rosenlof, K. H., and Kley, D.: The increase in stratospheric water vapour from balloonborne, frostpoint hygrometer measurements at Washington D.C. and Boulder, *Geophys. Res. Lett.*, 27, 3453–3456, 2000.
- 30 Peter, Th., Luo, B. P., Wirth, M., Kiemle, C., Flentje, H., Yushkov, V. A., Khattatov, V., Rudakov, V., Thomas, A., Borrmann, S., Toci, G., Mazzinghi, P., Beuermann, J., Schiller, C., Cairo, F., Di Donfrancesco, G., Adriani, A., Volk, C. M., Ström, J., Noone, K., Mitev, V., MacKenzie, R. A., Carslaw, K. S., Trautmann, T., Santacesaria, V., and Stefanutti, L.: Ultrathin Tropical

Tropopause Clouds (UTTCs): I. Cloud morphology and occurrence, *Atmos. Chem. Phys.*, 3, 1083–1091, 2003,

<http://www.atmos-chem-phys.net/3/1083/2003/>.

Schiller, C., Krämer, M., Afchine, A., Spelten, N. and Sitnikov, N.: The ice water content in Arctic, mid latitude and tropical cirrus, *J. Geophys. Res.*, doi:10.1029/2008JD010342, in press, 2008.

Schröder, F., Kärcher, B., Duroure, C., Ström, J., Petzold, A., Gayet, J. F., Strauss, B., Wendling, P., and Borrmann, S.: On the transition of contrails into cirrus clouds, *J. Atmos. Sci.*, 57, 464–480, 2000.

Seifert, M., Ström, J., Krejci, R., Minikin, A., Petzold, A., Gayet, J.-F., Schlager, H., Ziereis, H., Schumann, U., and Ovarlez, J.: Aerosol-cirrus interactions: a number based phenomenon at all?, *Atmos. Chem. Phys.*, 4, 293–305, 2004, <http://www.atmos-chem-phys.net/4/293/2004/>.

Sherwood, S. C. and Dessler, A. E.: A Model for transport across the tropical tropopause, *J. Atmos. Sci.*, 58, 765–779, 2001.

Sitnikov, N. M., Yushkov, V. A., Afchine, A. A., Korshunov, L. I., Astakov, V. I., Ulanovskii, A. E., Krämer, M., Mangold, A., Schiller, C., and Ravegnani, F.: The FLASH instrument for water vapor measurements on board the high altitude airplane, *Instrum. Exp. Tech.*, 50, 113–121, 2007.

Stephens, G. L. and Webster, P. J.: Clouds and climate: sensitivity of simple systems, *J. Atmos. Sci.*, 38, 235–247, 1981.

Strapp, J. W., Albers, F., Reuter, A., Korolev, A. V., Maixner, U., Rashke, E., and Vukovic, Z.: Laboratory measurements of the response of a PMS OAP-2DC, *J. Atmos. Oceanic Technol.*, 18, 1150–1170, 2001.

Ström, J., Strauss, B., Anderson, T., Schröder, F., Heintzenberg, J., and Wendling, P.: In-situ observations of the microphysical properties of young cirrus clouds, *J. Atmos. Sci.*, 54, 2542–2553, 1997.

Thomas, A., Borrmann, S., Kiemle, C., Cairo, F., Volk, M., Beuermann, J., Lepuchov, B., Santacesaria, V., Matthey, R., Rudakov, V., Yushkov, V., MacKenzie, A. R., and Stefanutti, L.: In-situ measurements of background aerosol and subvisible cirrus in the tropical tropopause region, *J. Geophys. Res.*, 107, 4763, doi:10.1029/2001JD001385, 2002.

Vaughan, G., Schiller, C., MacKenzie, A. R., Bower, K., Peter, T., Schlager, H., Harris, N. R. P., and May, P. T.: SCOUT-O<sub>3</sub>/ACTIVE high-altitude aircraft measurements around deep tropical

**Ice particles in the tropical stratosphere**

M. de Reus et al.

Title Page

Abstract

Introduction

Conclusions

References

Tables

Figures

◀

▶

◀

▶

Back

Close

Full Screen / Esc

Printer-friendly Version

Interactive Discussion



convection, B. Am. Meteor. Soc., 89, 647–662, 2008.

Voigt, C., Schlager, H., Ziereis, H., Kärcher, B., Luo, B. P., Schiller, C., Krämer, M., Popp, P. J., Irie, H., and Kondo, Y.: Nitric acid uptake in cirrus clouds, Geophys. Res. Lett., 33, L05803, doi:10.1029/2005GL025159, 2006.

5 Yushkov, V., Oulanovsky, A., Lechenuk, N., Roudakov, I., Arshinov, K., Tikhonov, F., Stefanutti, L., Ravegnani, F., Bonafe, U., and Georgiadis, T.: A chemiluminescent analyzer for stratospheric measurements of the ozone concentration (FOZAN), J. Atmos. Oceanic Technol., 16, 1345–1350, 1999.

10 Zöger, M., Afchine, A., Eicke, N., Gerhards, M. T., Klein, E., McKenna, D. S., Mörschel, U., Schmidt, U., Tan, V., Tuitjer, F., Woyke, T., and Schiller, C.: Fast in-situ stratospheric hygrometers: A new family of balloonborne and airborne Lyman- $\alpha$  photofragment fluorescence hygrometers, J. Geophys. Res., 104, 1807–1816, 1999.

ACPD

8, 19313–19355, 2008

## Ice particles in the tropical stratosphere

M. de Reus et al.

Title Page

Abstract

Introduction

Conclusions

References

Tables

Figures

◀

▶

◀

▶

Back

Close

Full Screen / Esc

Printer-friendly Version

Interactive Discussion



## Ice particles in the tropical stratosphere

M. de Reus et al.

**Table 1.** Number concentration (N), mean mode diameter (Dp) and standard deviation ( $\sigma$ ) for the two/three modal lognormal fitted size distributions. Note that the lognormal distribution is fitted to the median normalised size distribution shown in Fig. 2, while the number concentration in each mode is then scaled to the median number concentration which is actually observed in the specified potential temperature bin.

	N (cm <sup>-3</sup> )	Dp ( $\mu$ m)	$\sigma$
>385 K	0.044	9	1.55
	0.008	25	1.55
	0.0004	65	1.75
365–385 K	0.060	6	1.55
	0.0007	18	1.55
355–365 K	0.034	9	1.55
	0.0009	25	1.55
345–355 K	0.167	10	1.55
	0.026	35	1.55
	0.004	90	1.75

Title Page

Abstract

Introduction

Conclusions

References

Tables

Figures

I◀

▶I

◀

▶

Back

Close

Full Screen / Esc

Printer-friendly Version

Interactive Discussion



## Ice particles in the tropical stratosphere

M. de Reus et al.

**Table 2.** Average values of different meteorological variables and parameters derived from the ice crystal size distribution during the time periods in which ice crystals were observed in the stratosphere (the number of the event corresponds to the number in Fig. 6).

	1	2	3	4	5	6
Altitude (km)	18.0	18.0	18.4	18.4	18.7	18.2
Temperature (°C)	−81.7	−87.1	−83.9	−84.1	−80.9	−83.2
Pressure (hPa)	78.3	77.6	72.1	72.8	68.3	74.8
Pot. Temp. (K)	396	386	401	399	414	398
RHi (%)	76	157	95	107	75	89
N (cm <sup>−3</sup> )	0.10	0.30	0.015	0.048	–	0.050
IWC <sup>1</sup> (μg L <sup>−1</sup> )	1.7	0.89	0.19	0.084	–	0.33
IWC <sup>2</sup> (μg L <sup>−1</sup> )	1.3	0.99	0.16	0.16	0.072	0.40
<i>R</i> <sub>eff</sub> (μm)	25.4	17.9	23.6	11.5	–	19.5
<i>R</i> <sub>mean</sub> (μm)	9.3	4.6	7.7	5.1	–	7.1

<sup>1</sup> IWC derived from the observed ice crystal size distribution

<sup>2</sup> IWC derived from the two hygrometer measurements

Title Page

Abstract

Introduction

Conclusions

References

Tables

Figures

I◀

▶I

◀

▶

Back

Close

Full Screen / Esc

Printer-friendly Version

Interactive Discussion



## Ice particles in the tropical stratosphere

M. de Reus et al.

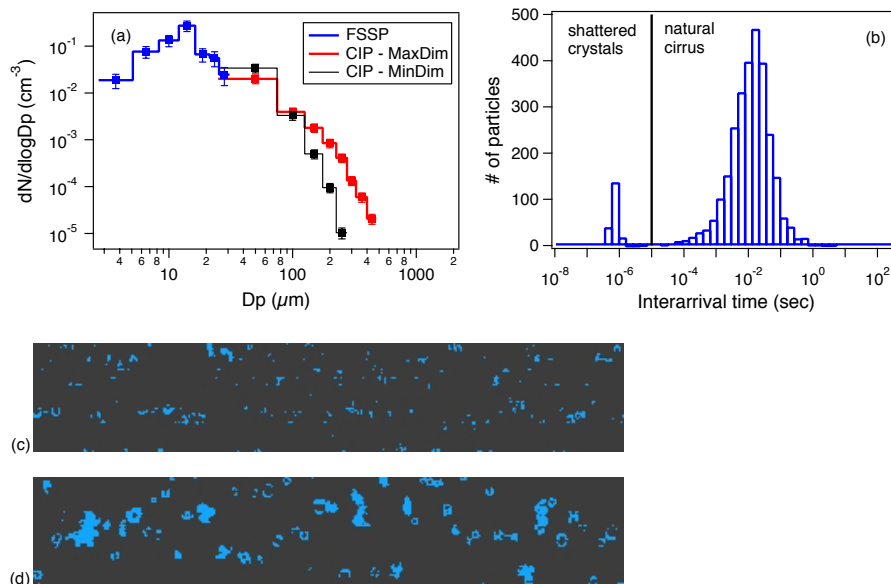


**Fig. 1.** (a) Ice crystal size distribution observed in the tropical stratosphere, 0.7 km above the local tropopause, over the Tiwi islands on 30 November 2005 (event 1 in Fig. 6). The ice crystal size distribution has been composed from FSSP and CIP data. For the CIP data the maximum and minimum dimension are shown. (b) Interarrival time distribution for the ice crystals observed by the CIP for this time period, indicating the crystals which are produced by shattering and therefore have been removed from the data set. (c) Ice crystal images recorded by the CIP instrument for this time period. (d) Example of larger ice crystals observed on 28 November 2005 at 10 km altitude.

[Title Page](#)
[Abstract](#)
[Introduction](#)
[Conclusions](#)
[References](#)
[Tables](#)
[Figures](#)
[I◀](#)
[▶I](#)
[◀](#)
[▶](#)
[Back](#)
[Close](#)
[Full Screen / Esc](#)
[Printer-friendly Version](#)
[Interactive Discussion](#)


Ice particles in the  
tropical stratosphere

M. de Reus et al.

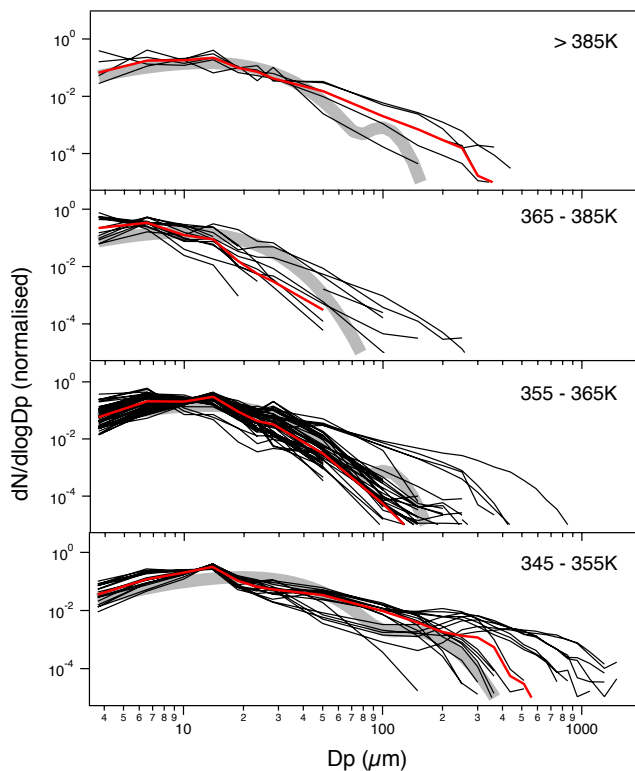


**Fig. 2.** Normalised ice crystal size distributions of the selected cirrus events (black lines). The median observed size distribution is included as red line. For clarity no error bars are shown and no information about the overlapping size region of FSSP and CIP. This has been shown for a selected size distribution in Fig. 1. The thick grey line shows the ice crystal size distribution calculated using the parameterisation of McFarquhar and Heymsfield (1997) for the average IWC and ambient temperature in the different potential temperature bins.

[Title Page](#)[Abstract](#)[Introduction](#)[Conclusions](#)[References](#)[Tables](#)[Figures](#)[◀](#)[▶](#)[◀](#)[▶](#)[Back](#)[Close](#)[Full Screen / Esc](#)[Printer-friendly Version](#)[Interactive Discussion](#)

## Ice particles in the tropical stratosphere

M. de Reus et al.

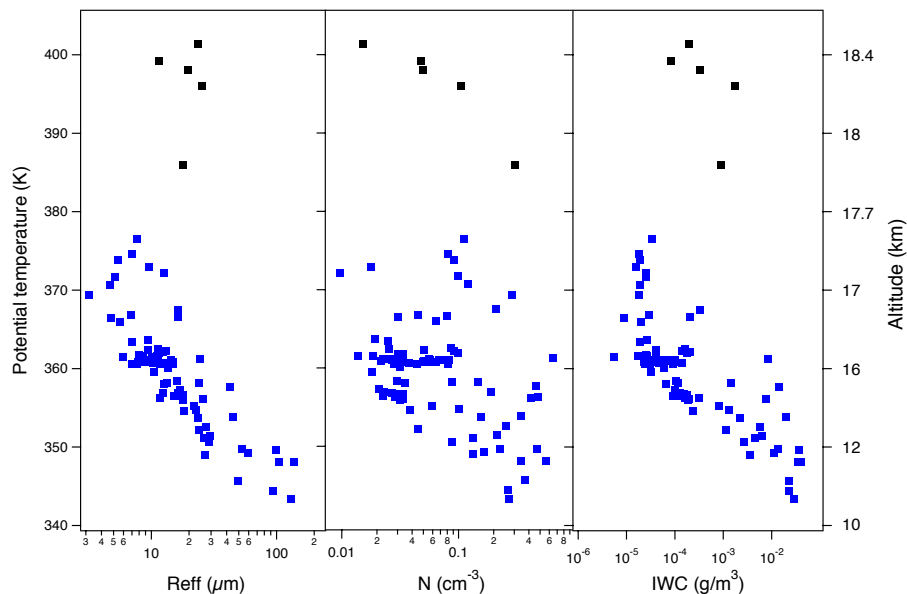


**Fig. 3.** The effective radius ( $R_{\text{eff}}$ ), ice crystal number concentration ( $N$ ) and ice water content (IWC) calculated from the ice crystals size distribution presented in Fig. 2. The black markers indicate the ice crystals observed in the stratosphere over the Hector storm system. On the right axis the approximate altitude is shown corresponding to the potential temperature on the left axis.

[Title Page](#)[Abstract](#)[Introduction](#)[Conclusions](#)[References](#)[Tables](#)[Figures](#)[◀](#)[▶](#)[◀](#)[▶](#)[Back](#)[Close](#)[Full Screen / Esc](#)[Printer-friendly Version](#)[Interactive Discussion](#)

Ice particles in the  
tropical stratosphere

M. de Reus et al.

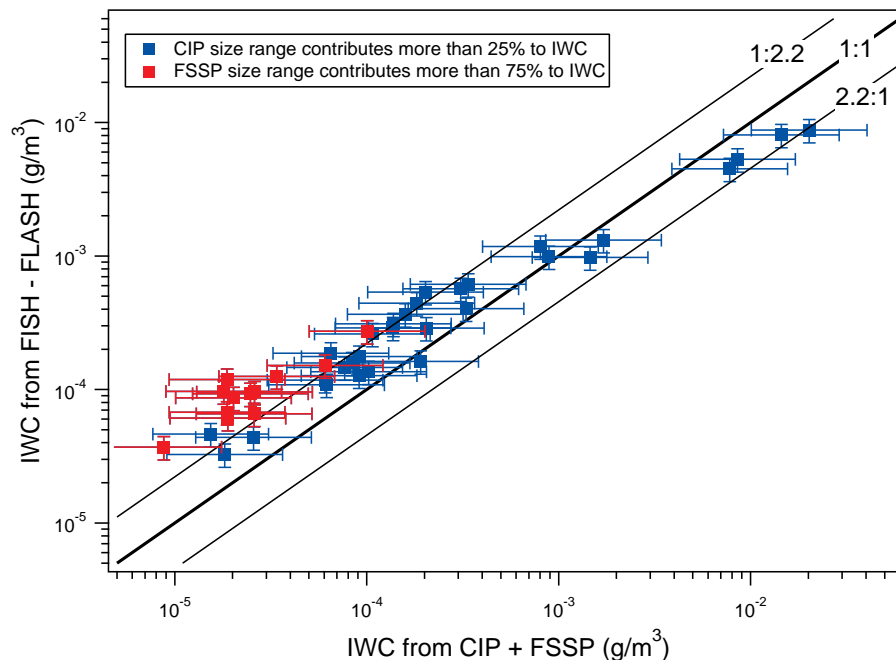


**Fig. 4.** Comparison of the ice water content derived from the size distribution measurements to the IWC obtained from the hygrometer instruments. The thin solid lines represent a deviation from the 1:1 line (thick solid line) with a factor 2.2, which corresponds to the combined uncertainty of both methods. The data points shown in this figure are averages over at least 30 s and correspond to the ice cloud encounters on 29 and 30 November (double flight) shown in Fig. 3.

[Title Page](#)[Abstract](#)[Introduction](#)[Conclusions](#)[References](#)[Tables](#)[Figures](#)[◀](#)[▶](#)[◀](#)[▶](#)[Back](#)[Close](#)[Full Screen / Esc](#)[Printer-friendly Version](#)[Interactive Discussion](#)

Ice particles in the  
tropical stratosphere

M. de Reus et al.

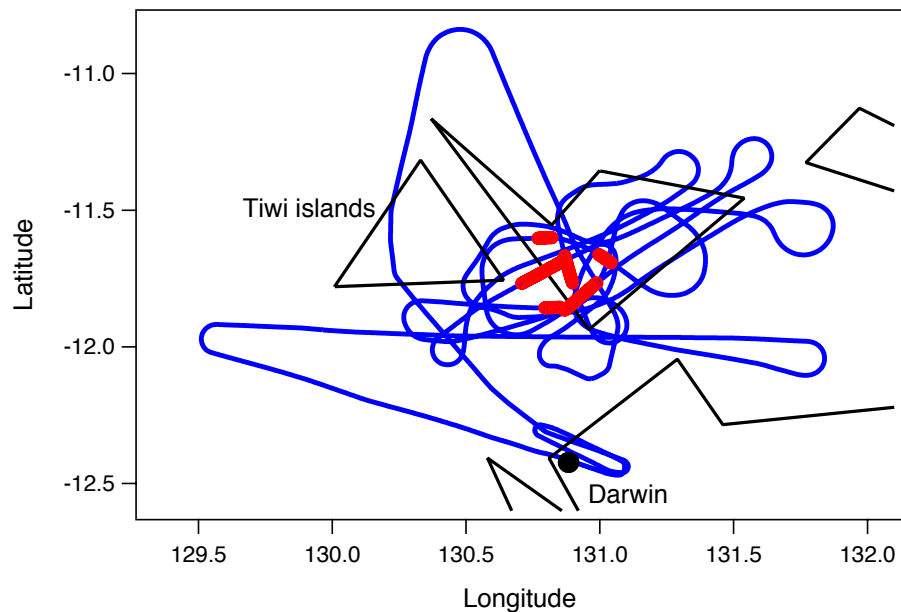


**Fig. 5.** Flight track of the M55-Geophysica on 30 November 2005. The red symbols indicate the geographical position where the ice crystals were observed in the stratosphere.

[Title Page](#)[Abstract](#)[Introduction](#)[Conclusions](#)[References](#)[Tables](#)[Figures](#)[◀](#)[▶](#)[◀](#)[▶](#)[Back](#)[Close](#)[Full Screen / Esc](#)[Printer-friendly Version](#)[Interactive Discussion](#)

## Ice particles in the tropical stratosphere

M. de Reus et al.

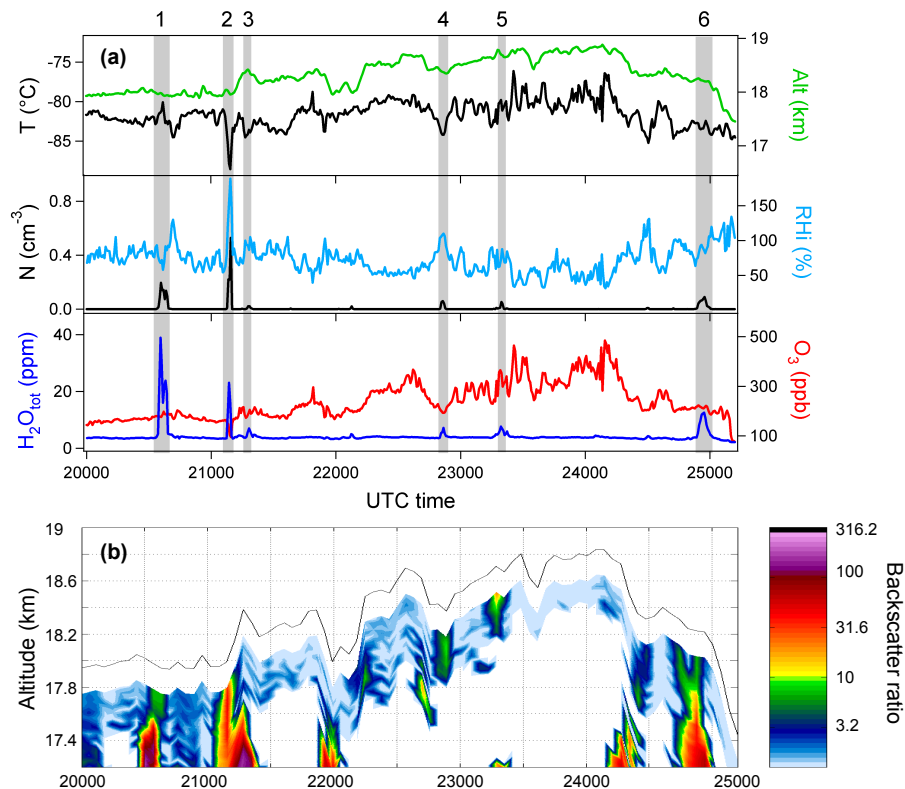


**Fig. 6.** (a) Ten second averaged values of the temperature, altitude, relative humidity, ice crystal number concentration ( $N$ ), total water content ( $\text{H}_2\text{O}_{\text{tot}}$ ) and  $\text{O}_3$  mixing ratio during the stratospheric part of the flight on 30 November 2005. (b) Backscatter ratio below the aircraft as measured by the downward looking lidar. The black solid curve is the flight altitude.

[Title Page](#)
[Abstract](#)
[Introduction](#)
[Conclusions](#)
[References](#)
[Tables](#)
[Figures](#)
[◀](#)
[▶](#)
[◀](#)
[▶](#)
[Back](#)
[Close](#)
[Full Screen / Esc](#)
[Printer-friendly Version](#)
[Interactive Discussion](#)


Ice particles in the  
tropical stratosphere

M. de Reus et al.

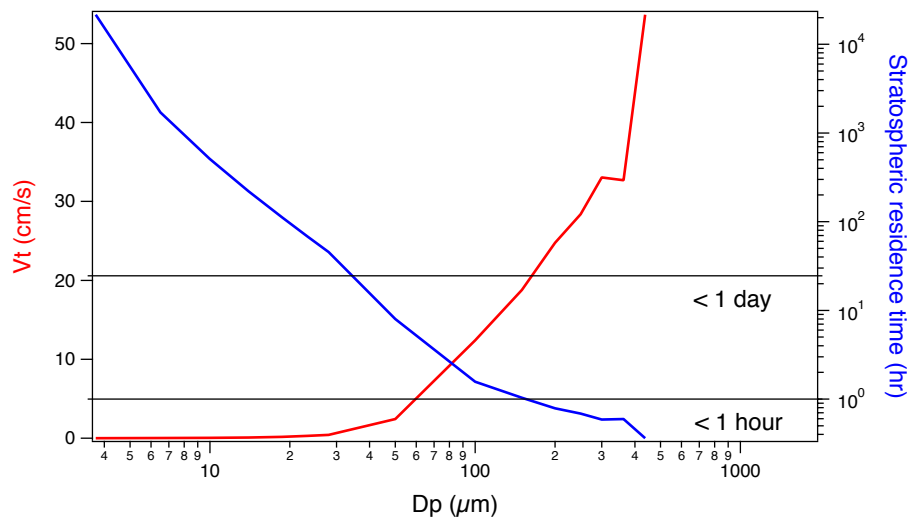


**Fig. 7.** Gravitational settling velocity ( $V_t$ ) and stratospheric residence time for the ice crystals observed in event 1 of Fig. 6 assuming an altitude above the tropopause of 0.7 km.

[Title Page](#)[Abstract](#)[Introduction](#)[Conclusions](#)[References](#)[Tables](#)[Figures](#)[◀](#)[▶](#)[◀](#)[▶](#)[Back](#)[Close](#)[Full Screen / Esc](#)[Printer-friendly Version](#)[Interactive Discussion](#)

## Ice particles in the tropical stratosphere

M. de Reus et al.

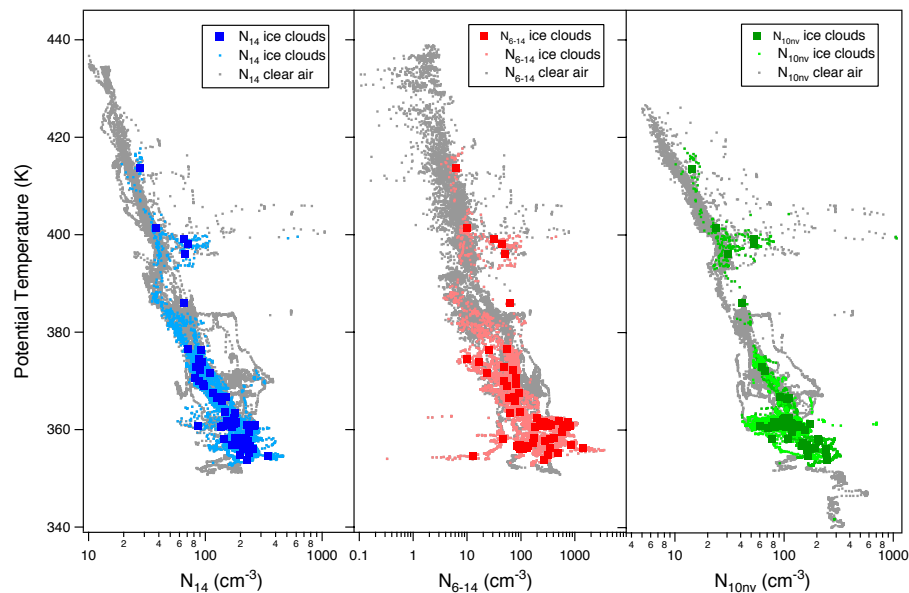


**Fig. 8.** Profiles of the total, ultrafine and non-volatile aerosol number concentration for in (coloured dots) and out of cloud (grey dots) measurements. The markers indicate the average interstitial aerosol number concentration within the selected ice clouds.

[Title Page](#)[Abstract](#)[Introduction](#)[Conclusions](#)[References](#)[Tables](#)[Figures](#)[◀](#)[▶](#)[◀](#)[▶](#)[Back](#)[Close](#)[Full Screen / Esc](#)[Printer-friendly Version](#)[Interactive Discussion](#)

## Ice particles in the tropical stratosphere

M. de Reus et al.

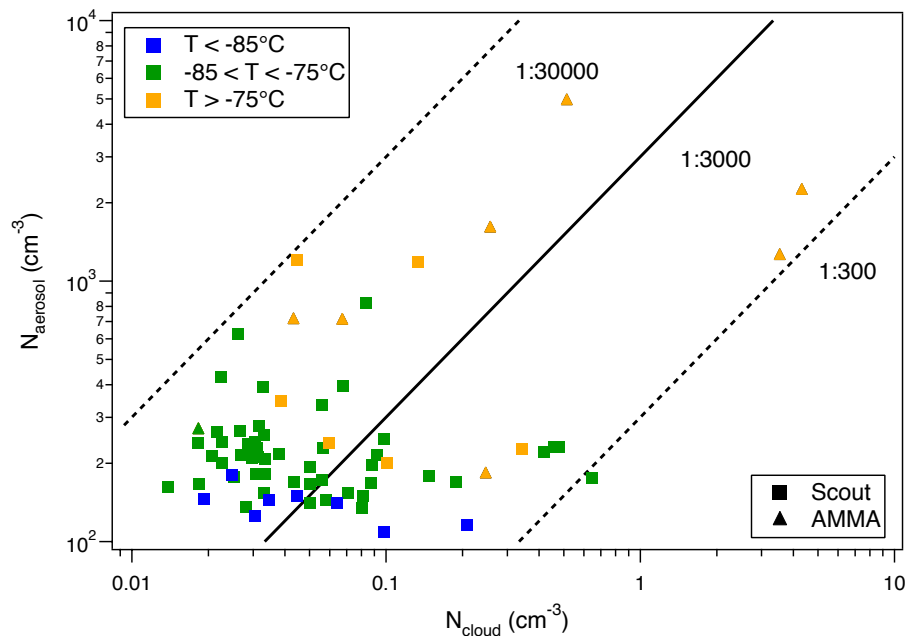


**Fig. 9.** Interstitial aerosol number concentration as function of the ice crystal number concentration for three temperature ranges. The data points (squares) shown in this figure are averages over at least 30 s and correspond to the ice cloud encounters during the SCOUT campaign shown in Fig. 3. The triangles are ice cloud encounters at similar ambient temperatures during the AMMA (African Monsoon Multidisciplinary Analyses) campaign over West Africa in August 2006.

[Title Page](#)[Abstract](#)[Introduction](#)[Conclusions](#)[References](#)[Tables](#)[Figures](#)[I◀](#)[▶I](#)[◀](#)[▶](#)[Back](#)[Close](#)[Full Screen / Esc](#)[Printer-friendly Version](#)[Interactive Discussion](#)

Ice particles in the  
tropical stratosphere

M. de Reus et al.

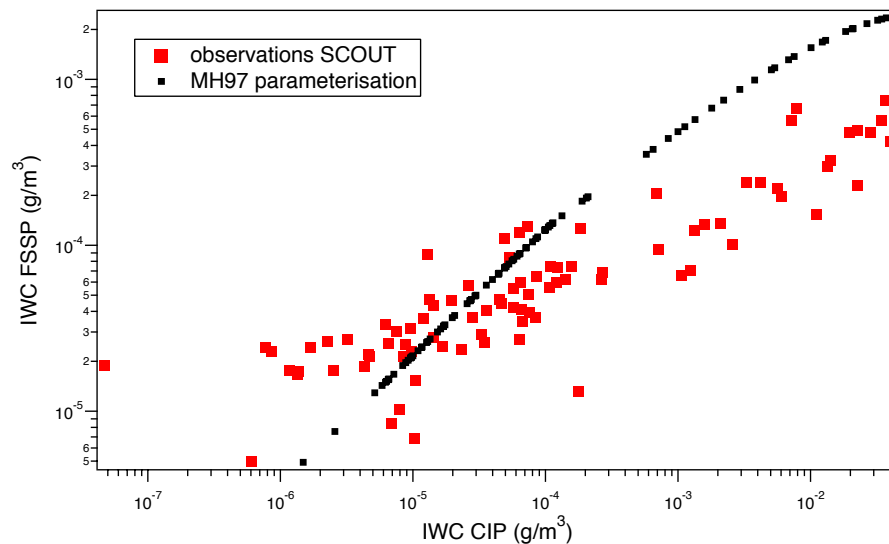


**Fig. 10.** Comparison of the ice water content measured by the FSSP and CIP instruments to the IWC for the same size ranges calculated using the parameterisation of McFarquar and Heymsfield (1997).

[Title Page](#)[Abstract](#)[Introduction](#)[Conclusions](#)[References](#)[Tables](#)[Figures](#)[I◀](#)[▶I](#)[◀](#)[▶](#)[Back](#)[Close](#)[Full Screen / Esc](#)[Printer-friendly Version](#)[Interactive Discussion](#)